The impact of tectonic-style on marine transgression and evolution

D. S. Stevenson [ID]

Carlton le Willows Academy, Wood Lane, Gedling, Nottingham NG4 4AA, UK

Abstract

Plate tectonics drives variation in sea-level, over intervals of approximately 10^7–10^8 years. These variations may have significant effects on the pace of (biological) evolution through the elimination of terrestrial niches and the expansion of shallow-water marine niches. However, within the solar system, only the Earth experiences this kind of tectonism. Venus displays regional tectonism, characterized by rising diapirs within the plastic mantle. Impinging on the lithosphere, these plumes produce a range of structures of varying dimensions; the uplift of which would raise sea-level, were Venus to have oceans. Using Magellan observations of Venus, we model the impact of regional tectonism on sea-level for given areas of Venusian ocean, then compare the effect with terrestrial tectonic processes for similar oceanic area. We show that despite variation in the geographical extent of Venusian-style tectonic processes, the styles of regional tectonism on Venus can produce the same order of magnitude changes in sea-level, for a given area of ocean, as plate tectonics. Consequently, we examine some of the impacts of marine transgression on habitability and the evolution of life.

Introduction

Terrestrial plate tectonics affords our planet with many properties which are advantageous for the development and subsequent evolution of life (Zahnle et al., 2007; Dohm and Maruyama, 2015). However, plate tectonics appears to have begun on Earth perhaps as late as 2 billion years after the Earth's formation and perhaps 0.5–1.0 billion years after life began (Bindeman et al., 2018; Cawood et al., 2018). It is now, generally, assumed that prior to its inception, terrestrial tectonism was likely regional in extent and perhaps more akin to that, currently, observed on Venus (Rozel et al., 2017). Therefore, plate tectonics does not appear to have been necessary for the inception of life on Earth.

Irrespective of its role in life's inception, there are a significant number of evolutionary innovations that appear tied to the operation of plate tectonics. We know, for example, that the Cambrian Explosion (Budd and Jackson, 2016; Landing and Kouchinsky, 2016) occurred to the back-drop of extensive marine transgressions on Earth (Brasier, 1980, 1982; Banerjee et al., 1997; Banerjee and Mazumdar, 1999; Squire et al., 2006; Peters and Gaines, 2012; Landing and Kouchinsky, 2016; Clemmensen et al., 2017; Karlstrom et al., 2018; Latif et al., 2018; Paterson et al., 2019; Wei et al., 2018) and that various extinction events are associated with transgressions during the Phanerozoic (Bond and Wignall, 2008; Munnecke et al., 2010; Vodráqková et al., 2013; Barash, 2014; Brocke et al., 2015; Percival et al., 2018; Williams et al., 2019). For example, extinction in the Devonian is linked to eutrophication and anoxia in the so-called Basal Choteč Event (Vodráqková et al., 2013).

Such transgressions, where the oceans inundate extensive areas of continental crust, are caused by a variety of geological processes, including the formation of new, buoyant oceanic crust (Zhong et al., 2007; Müller et al., 2008); the extrusion of lavas to form Large Igneous Provinces (LIPs, Coffin and Eldholm, 1994; Gladczenko et al., 1997; Müller et al., 2008) and the subsidence of passive continental margins (Müller et al., 2008; Kirschner et al., 2010; Conrad, 2013; Sim et al., 2016). For example, the opening of the central Atlantic Ocean, 180 million years ago, is thought to have raised global sea-levels by 30–50 m as new, buoyant ocean crust was produced (Conrad, 2013). Indeed, with the exception of climate-driven changes in sea-level, such as Milanković-cycle-driven events, tectonism has the largest contribution to terrestrial sea-level changes on 10^7–10^8-year timescales (Conrad, 2013). As Earth is the only known world with plate tectonics, we wanted to consider whether regional tectonism, of the kind seen on Venus, could drive similar magnitudes of change in sea-level.

While marine transgressions are a general feature of the Phanerozoic (and likely earlier in terrestrial history), the impact these have had on the terrestrial biosphere has varied with the biological context. Perhaps the most extensively studied are the series of Cambrian-early Ordovician transgressions. During the latest Proterozoic, very extensive (and perhaps glacial) denudation of all (or at least most) the continental platforms is seen (Keller et al., 2019). This event erased much of the continental surface. Subsequently, during the Cambrian era, oceans

flooded extensive areas of continental crust, including Laurentia (Brasier, 1980; Karlstrom et al., 2018; Keller et al., 2019), Avalonia and Baltica (Brasier, 1980, 1982), India (Banerjee et al., 1997; Banerjee and Mazumdar, 1999), the Chinese platforms (Wei et al., 2018). In Laurentia, marine transgressions extended over two-thirds of the continent. Here, the advancing shoreline is associated with wave-driven incision ('razoring') of the rock and soil delivers a large nutrient burden to the oceans (Peters and Gaines, 2012).

Deep-water anoxia is also recorded in a number of global locations and may be associated with an increase in the availability of nutrients in the top layers of the ocean, leading to eutrophication. Although not proven, there is the suggestion that alteration in nutrient supply, and associated deep-water anoxia, may have led to the extinction of some Ediacaran biotas, and the opening up of niches for Cambrian fauna (Wei et al., 2018). The period of greatest evolutionary diversification occurs in a window spanning 540–521 million years ago, throughout the early Cambrian, with further waves of diversification immediately prior to and subsequent to this period (Paterson et al., 2019). Paterson et al. (2019) show through statistical analysis of the pattern of radiation, that the Cambrian Explosion represents radiation of crown phyla which had begun to diversify in the Ediacaran (Wood et al., 2019). Similarly, Lee et al. (2013) use similar Bayesian analysis to show that diversification happened throughout the early Cambrian, but critically, that this process represents a 5.5-fold acceleration in the phylogenetic diversification rate and a four-fold diversification in the phenotypic rate, as compared to later Phanerozoic periods.

Similarly, during the Ordovician and Devonian eras, repeated transgressions are associated with regional extinction events and the introduction of new fauna (Becker et al., 2016; Bond and Wignall, 2008; Munnecke et al., 2010; Vodráqková et al., 2013; Barash, 2014; Brocke et al., 2015; Colmenar and Rasmussen, 2017; Percival et al., 2018; Williams et al., 2019). Extinction is through the loss of habitat and, at least in some circumstances, the spread of anoxic sea waters over continental margins (Vodráqková et al., 2013; Brocke et al., 2015; Percival et al., 2018). Novel species then evolve to fill the available niches on the new, shallow continental margins, or colonize land when marine regression occurs. The Cambrian Explosion is principally an innovation of marine species (e.g. López-Villalta, 2016), which would be expected if a large number of euphotic and nutrient-rich habitats became available.

Cambrian speciation was also favoured because it was coupled with the loss of competing Ediacaran species (Grazhdankin, 2004; Paterson et al., 2019). In many instances, the emergence of these new biotas is evident through bioturbation, where Cambrian fauna disturb the sediment on the ocean floor. Such structures are absent in the finely laminated Ediacaran record, which suggests that increases in oxygen content of the ocean and sedimentary layers allowed animals to burrow (e.g. Fox, 2016).

While there are likely multiple causes for the Cambrian and Ordovician radiations (reviewed in Fox, 2016), changes to the environment critically affect the abundance of habitats and the energy available to organisms. During the latest Ediacaran and early Cambrian, the opening of the complex Iapetus Ocean basin would have raised sea-levels by tens of meters, with the value varying with the total length of ridge associated with this geological event (Cawood et al., 2001; Hodych and Cox, 2007; Domeier, 2016). Production of buoyant lithosphere drove seawaters several hundred kilometres inland, over the denuded

Ediacaran-early Cambrian landscape (Hoffman et al., 2011; Keller et al., 2019). Similarly, during the early Ordovician radiation, the opening of the Rheic Ocean was associated with diversification of the biota (Colmenar and Rasmussen, 2017), emphasising the role of tectonism in evolutionary diversification. The late Proterozoic glaciations would not only denude the landscape, but produce a wealth of nutrient-rich ground rock and dust, which would be available to the oceans upon transgression. For every rise of 1 m in terrestrial sea-level, there is a 10 m retreat of the shoreline (Zhang et al., 2004), ensuring that even modest sea-level rises can lead to the significant retreat of any shoreline. Transgression then opened up countless new niches for life that occupied these empty, potential habitats, or colonized those vacated by Ediacaran biotas.

Peters and Gaines (2012) make a strong case for marine transgression as a driver of the Cambrian explosion. Their argument rests on two changes: the increased supply of nutrients and the mobilization of the glaciated regolith that followed late Neoproterozoic glaciations (Peters and Gaines, 2012; Keller et al., 2019). Moreover, we can add a further couple of biological queues: increases in the abundance of high-energy, euphotic environments, in which marine organisms could exist; and the impact of a well-known biological relationship – the species–area relationship (SAR; Lomolino, 2000; Stevenson and Wallace, 2021, in press). In the case of the former, the emergence of an abundance of shallow, marine environments will allow the proliferation of food-chains driven by photosynthetic producers. In the case of the latter, more shallow marine environments allow more species to exist. In each case, the proliferation of extant species in new areas allows for the evolution of novel species through allopatric speciation (Gray, 2001; Heenan and McGlone, 2013; Rahbek et al., 2019).

While additional factors, such as enhanced volcanism, clearly contribute to mass extinction events (Barash, 2014), there is ample evidence that changes in sea-level are drivers of extinction events, through the mechanisms discussed previously (Vodráqková et al., 2013; Barash, 2014). For example, Barash (2014) links the effect of global cooling and glaciation on sea-level regression, to the loss of shallow marine habitats in the Ordovician extinction; while Vodráqková et al. (2013) show increases in nutrient supply and eutrophication during transgression lead to extinction in the Devonian.

In this paper, we ask whether regional Venusian tectonic processes would be sufficient to produce significant marine transgressions and, therefore, the kinds of evolutionary diversification seen on Earth. Briefly, we also consider how variation in sea-level can influence the rate of erosion, planetary albedo and the delivery of nutrients to the oceans. We accept that tectonism has a role subordinate to the effects of ingassing and degassing over hundred million to billion year-timescales in driving sea-level change (Kasting and Holm, 1992; Korenaga, 2011; Conrad, 2013). However, we show that over 10^7–10^8-year timescales, regional tectonism can be a significant driver of sea-level change on planets that experience it. Hence, these planets will also experience the kinds of environmental changes that promote evolutionary diversification.

Methods

The method is split into two sections. In the first, we discuss the range of factors that are known to affect sea-level and their approximate timescales; then in the second, we focus on the

methodology of determining sea-level changes associated with tectonic events.

Rationale

In this section of the paper, we provide a rationale for the model employed and compare the model with other factors that influence sea-level on terrestrial planets.

Temporal relationships of features and approximated rates of formation

Approximate ages of the three Venusian tectonic features are estimated relative to the wrinkled plains (Smrekar and Stofan, 1997; Basilevsky and Head, 1998a, 1998b; Krassilnikov and Head, 2003). The oldest features may be the large volcanic rises, based on their geospatial relationship to the coronae, which are in turn ages relative to the wrinkled plains (Basilevsky and Head, 1998a, 1998b). However, given the identification of active volcanism at some large rise volcanic centres, they have ages spanning a few hundred million years (Fig. 1). Overall, the coronae appear to have been emplaced in two phases. The first phase involving up-doming occurred prior to the wrinkled plains at around 350–300 million years ago, with volcanism, at these centres, occurring contemporaneously and subsequently to the wrinkle plains (Krassilnikov and Head, 2003).

Estimates of the novae ages suggest that while some formed at the same time as the coronae, most post-date the wrinkled plains, suggesting that these are younger overall (Krassilnikov and Head, 2003). Both the coronae and novae have been intruded over an interval of a few hundred million years, but the precise period is unknown. Therefore, in the absence of precise temporal information, we are forced to neglect direct dissection of the rate of change of sea-level. An assumption that half of the coronae are emplaced per 100 million years would be in keeping with the available (limited) data (Basilevsky and Head, 1998a, 1998b; Krassilnikov and Head, 2003). The timing of the novae emplacement rate would be similar (Krassilnikov and Head, 2003).

Tectonic influences on terrestrial sea-level

Both continental rifting and basin closure, with associated continental shortening, influence terrestrial sea-levels. Counterintuitively, rifting tends to reduce overall ocean basin width, by stretching and thinning the lithosphere, while overlaying this thinned lithosphere with sediment. Stretching of continents is offset by subduction, or by continental shortening, elsewhere. Rifting is thought to marginally reduce basin area by 3.3% and cause a potential rise of 20 m (Müller et al., 2008; Kirschner et al., 2010; Conrad, 2013). Conversely, the shortening of continents, during the Alpine-Himalayan orogeny, may have lowered sea-levels by 25 m, as ocean basins increased in area after the elimination of the Neo-Tethys (Conrad, 2013). While Venus has continent-like areas, with significant crustal shortening, the precise mode in which these structures were formed is unclear. Therefore, we cannot make direct comparisons with terrestrial features.

Sedimentation

Sedimentation rates are profoundly affected by the distance from the continental margin and the climate of the region. However, terrestrial deep-water sedimentation rates are fairly-well constrained. Typically, rates are of the order 0.1–30 m per million years, with a rate approximating 1.8 km^3 yr^{-1} globally (Lyle, 2015; Olson et al., 2016). Terrestrial sediment flux broadly balances the accretion of material to continents during collisional events and brings the mean elevation of the continents close to sea-level (Olson et al., 2016). There is considerable variation from 11.4 m per million years at the North Atlantic margin to 1.2 m per million years along the North Pacific margins (Olson et al., 2016). On planets lacking plate tectonics, presumably ocean basins would slowly fill with sediment at a rate approximating 10^0–10^1 km^3 yr^{-1}. The precise value will depend on the relative area of land and sea areas, as well as regional and global climate.

Determining the effect on sea-level is complex. Aside from the considerations of isostatic compensation, influx would cause a progressive infilling of the basins and slow sea-level rise in the range of 10^{-2}–10^0 m per million years, depending on the volume and area of the ocean basin and the supply of sediments by erosion and biological activity. Slow rises would cause progressive transgression, which depending on the hypsometric curve of the planet ultimately reduce erosion rates by reducing the available surface on which weathering and erosion can act. The effect would be subsequent to the initial effect of razoring, by the advancing seafront (next section).

Effect of sea-level rise on coastal erosion rate

There are two potential effects of sea-level rise on the rate of erosion. Firstly, variation in ocean depth would be expected to alter the available gravitational potential across drainage systems. A reasonable expectation might be that a lowering of ocean depth, relative to the level of the continental platform, would result in a steepening of the gradient of river systems and a significant increase in the rate of erosion. In turn, a higher rate of erosion could increase the delivery of nutrients to the ocean. Duran et al. (2019) identify 'knickpoints' in Martian fluvial channels, which appear analogous to headwalls in terrestrial river channels, where a steepening of the gradient has caused retreat of the base of the river channel. In the Martian case, these headwalls area is associated with reductions in sea-level and an increase in the gravitational potential energy in the fluvial system.

Terrestrial erosion rates can be measured with beryllium-10 (^{10}B) production through cosmic ray spallation of nitrogen and oxygen nuclei. Portenga and Bierman (2011) show that while slope gradient has a high correlated relationship with erosion rate, elevation, per se, does not. Therefore, for the purposes of this paper, we do not expect a significant variation in the rate of erosion for variations in altitude relative to sea-level.

However, such minor variation should be contrasted with razoring of shorelines, as sea-levels rise. Terrestrial erosion rates along shorelines are positively correlated with increases in sea-level (Zhang, 1998; Zhang, et al., 2004). Enhancement of erosion rate is likely a consequence of waves being able to act further up the beach profile and remove sediment (Zhang et al., 2004). Therefore, we expect increases in sea-level to show a marked positive correlation with erosion and the supply of nutrients to the oceans. The overall rate of coastline retreat is correlated with the sea-level rise through equation (1).

$$s(D_B + D_C) = \text{active profile slope, } a = \frac{(D_B + D_C)}{l}s. \quad (1)$$

Here, s is shoreline recession, D_B is the elevation of the shore above sea-level, D_C is the depth of closure, a is the rise of sea-level and l is the distance from the shore to the 'closure point'. The closure point is the most landward depth on the sea floor, seaward

Fig. 1. Approximate formation and activity periods for novae, coronae and large volcanic rises. Krasslinikov and Head estimate 40% of novae formed before the wrinkled plains (PWR) approximately 300 million years ago, with the remainder forming after these structures (Krassilnikov and Head, 2003). The Coronae appear to have formed largely contemporaneously with the wrinkled plains but activity may have extended to a more limited extent until 100 million years ago (Basilevsky and Head, 1998a, 1998b). Formation of the large volcanic rises may predate the formation of coronae as many have coronae at their summits. Therefore, it is unclear if all of the rises have similar dates, or whether some are more recent (Smrekar and Stofan, 1997).
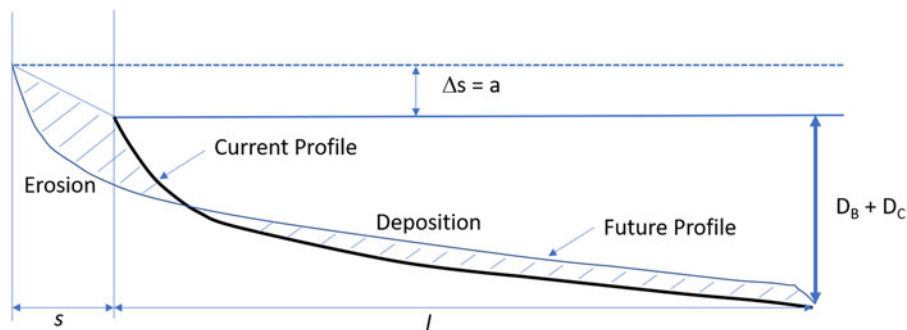
of which there is no significant change in the bottom elevation; and where there is no significant net sediment-exchange between the nearshore and the offshore. Equation (1), otherwise known as the Bruun equation, typically has a value of s/a of 50–100, or a coastal retreat on the order of two orders of magnitude greater than the sea-level rise (Zhang *et al.*, 2004). The components are illustrated in Fig. 2.

For the purposes of this paper, there are two considerations: Firstly, a consideration of the rate of transgression relative to the rate of sea-level rise; and secondly, the concomitant rate of razoring and nutrient delivery to the oceans. These will be considered, qualitatively, in the discussion. For the former, a rise of 100 m would lead to an erosive retreat approximating 10 000 m. However, the effect of erosive retreat is subordinate to the impact of the hypsometric curve. Given the terrestrial and Venusian hypsometric curves, after an initial rise and erosive burst, shorelines will retreat rapidly through simple flooding.

Contributions to sea-level change from aquifers

Sames *et al.* (2020) report that terrestrial contributions of aquifers to sea-level likely fall in the range of 0.04–0.7 mm yr^{-1}. While their influence could amount to a few meters over short intervals, determining an influence on other planets would be problematic. Variables, such as climate, rock type(s) and land area aquifer volume will vary considerably. Specifically, Sames *et al.* (2020) implicate climatic effects in Cretaceous sea-level change, linked to Milanković Cycles. Given wide-variation in the spin-orbital characteristics and axial inclination of different planets, we have chosen to neglect their contribution to aquifer loading and unloading and sea-level variation, in this instance.

Loss of water to space

Ocean depth will depend on the rate of loss of water to space. The rate of loss of volatiles to space is controlled by a number of factors, which include the escape velocity of the planet (which is planetary mass-dependent) and the temperature of the lower atmosphere (which is dependent on the orbital distance and stellar luminosity). Additional factors, such as tidal-heating, incident intensity of XEUV and atmospheric composition, will also influence the loss of volatiles (Bolmont *et al.*, 2017).

Such variables will vary from planet to planet and are difficult to control in this analysis. However, for the sake of completeness, we note that Martian losses are on the order of 38 m of surface water since the Noachian era (Carr and Head, 2015). Terrestrial losses are considerably lower, on the order of 9500 m^3 yr^{-1}, or a depth equivalent of 1.86×10^{-5} m yr^{-1}, when averaged over the entire surface. The low figure principally reflects the greater escape velocity of our planet, compared to Mars and the presence

of the tropospheric cold-trap. Over the time periods considered for the impact of tectonism (10^7–10^8 years), the impact of the loss of water to space is inconsequential for bodies with masses approximating the Earth and with terrestrial insolation. However, we note, that for planets, which orbit active red dwarf stars, such losses could be substantial over these timescales (Bolmont *et al.*, 2017; Wheatley *et al.*, 2017).

Degassing and regassing of the mantle

The terrestrial mantle has likely switched from one where degassing predominated to one where regassing (ingassing) dominates in the last 1–2 billion years (Korenaga *et al.*, 2017). Regassing is dominated by fluxes through subduction of wet sediment and hydrothermally-altered ocean crust. Present day subduction-related (net) ingassing accounts for 2–3×10^{11} kg yr^{-1} (Korenaga, 2011; Korenaga *et al.*, 2017), which would be sufficient to drain the 1.34×10^9 km^3 ocean-volume in a few billion years, given concurrent degassing through volcanism (7×10^{11} kg yr^{-1}; Korenaga, 2011; Kurokawa *et al.*, 2018). Planets lacking subduction would have much slower returns of water to their interior, principally through reactions between mafic igneous rocks and water, or through the formation of sediments, which are then buried.

Schaefer and Sasselov (2015) carried out the modelling of planets of different masses and different convective regimes. In principle, more massive planets degass, then ingas at faster rates than Earth-mass planets. However, all of these models assume plate tectonics, with water cycling into the mantle via subduction. Therefore, they are not directly applicable to stagnant-lid planets, like Venus. We, therefore, assume that after initial strong degassing from a magma ocean, degassing rates will be relatively low in the absence of plate tectonics.

Modelling

Terrestrial tectonic data

Tectonic influences on terrestrial ocean depth, both from the formation and age of ocean crust and from the formation of LIPs, are from Müller *et al.* (2008), Kirschner *et al.* (2010) and Conrad (2013).

Venusian tectonic data

Evaluations of the size and evolution of Venusian coronae are from Basilevsky and Head (1998a, 1998b), Grindrod and Trudi Hoogenboom (2006) and Krassilnikov and Head (2003). These authors assume that coronae formation preceded novae formation. However, for the purposes of this work, we are interested in determining how the volume of plume-related activity in this
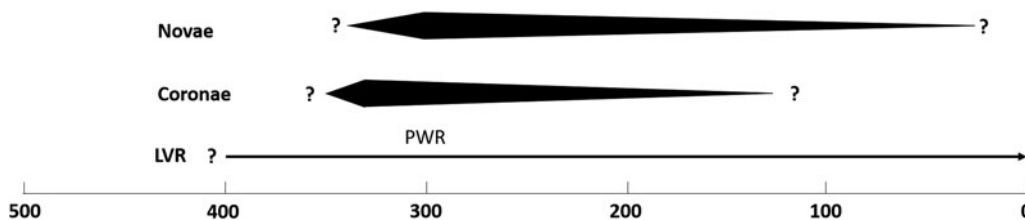
Fig. 2. Two-dimensional illustration of the components of the Brunn equation. The region of net erosion, length *s*, is equal to the area of net deposition, length *l*. These two areas are equal. The change in height, or active profile, is *a*, while DB and DC are the heights of net erosion and deposition. Modified from Zhang *et al.* (2004).

tectonic model relates to that produced in a terrestrial plate tectonic and plume setting, rather than their temporal relationship.

In terms of temporal relationships, formation of the large volcanic rises (below) likely precedes the coronae, as many (but not all) large volcanic rises have coronae on top of them. However, the precise ages are unclear. Smrekar and Stofan, (1997) assume that many large volcanic rises are still geologically active; therefore, their ages must extend from before the formation of the coronae that lie on them to the present day. The temporal relationship between the timescale of emplacement of novae and coronae was illustrated in Fig. 1. While the precise timing of their emplacement is currently unknown, it is thought both classes of the structure were constructed over a 100 million-year-long window (Basilevsky and Head, 1998a, 1998b; Krassilnikov and Head, 2003).

Approximating the volume of coronae and novae

Coronae come in a variety of different structural forms (Stofan *et al.*, 1992; Basilevsky and Head, 1998a, 1998b; Gridrod and Trudi Hoogenboom, 2006). The volume of coronae and novae was estimated using a simple cap volume calculation. Although this is a crude estimation, it does provide a ball-park estimate of the volume of an average corona and nova, which can then be used to determine the maximum displacement of ocean water.

There are approximately 514 coronae on the surface of Venus, with an uncertainty due to incomplete mapping by Magellan in the early 1990s (Squyres *et al.*, 1992; Stofan *et al.*, 1992; Gridrod and Trudi Hoogenboom, 2006; Kereszturi *et al.*, 2015). Similarly, novae are thought to number approximately 64, falling into various structural forms. These are reviewed in Krassilnikov and Head (2003). However, the general evolution of both coronae and novae is thought to involve an initial up-doming and accompanying volcanism that lasts for several tens of millions of years, to perhaps a couple of hundred million years (Basilevsky and Head, 1998a, 1998b). While both coronae and novae have a variety of structural forms, modelling coronae and novae as domes is a realistic approach given their structural evolution (Basilevsky and Head, 1998a, 1998b; Krassilnikov and Head, 2003).

The relevant volume, *v*, of coronae and novae was modelled as a simple cap, with mean values for diameter and height, using the following equation:

$$v = \frac{1}{6}\pi h(3a^2 + h^2), \qquad (2)$$

where *h* is the height of the dome and *a* is the radius (Fig. 3).

We appreciate that these calculations are a simplification; however, as the results are applied generally, we chose not to use specific morphologies of each corona, nova and large volcanic rise, as are found on Venus. Furthermore, we assume that the volume of the geological feature is not offset by the subsidence of the lithosphere
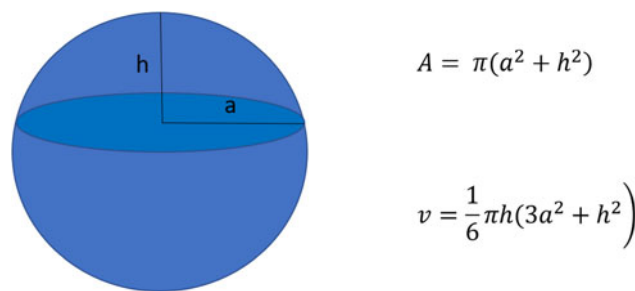

Fig. 3. Illustration of the cap calculation.

$$A = \pi(a^2 + h^2)$$

$$v = \frac{1}{6}\pi h(3a^2 + h^2)$$

under its weight. Finally, Venusian structures are clearly not underwater as equivalent structures are on Earth. Here, the weight of the overlying water would depress structures relative to their observed heights. To adjust for this effect, we assume that seawater has a density of approximately 30% that of mantle rock. Therefore, isostatic compensation (if complete) should cause observed sea-level change to be damped by a factor of 0.7 compared to changes in water-level thickness (Pitman, 1978; Conrad, 2013). All Venusian sea-level changes are, therefore, adjusted by multiplying by 0.7.

Similarly, for the sake of simplicity, ocean area and volume are modelled as follows. As ocean volume and area will vary from planet to planet, we produced three simple calculations to produce a proof-of-principle, only. Using Venus as our model, non-plate tectonic planet, oceans are assumed to fill one of the three scenarios: firstly, the lowlands and gently rolling uplands; secondly, the lowlands, alone; or finally, an area equivalent to the Earth's oceans. For the former scenario of lowlands, the oceans would have a depth of 1–2 km, and for the coverage of the lowlands and the gently rolling plains, a depth of 2–3 km (Rosenblatt *et al.*, 1994). These depths of ocean are obviously reasonable from a terrestrial stand-point; however, we cannot assume that other planets will have oceans of this depth. If they are shallower than 1 km in depth, then much of the structures we discuss will stand-proud of the surface of the ocean; therefore, the determined changes in sea-level will be an overestimate. Conversely, if the oceans are deeper than 12 km, then all Venusian structures will be drowned and these calculations are mute.

The specific areas of Venusian terrain are available from Magellan (Saunders *et al.*, 1992). The effect of corona or nova volume on ocean depth is derived simply by dividing the total volume of these structures (the sum of all of their volumes) by the surface area of the ocean. No further assumptions are made regarding any other processes, such as sedimentation, isostatic readjustment or changes to geoid height (Conrad, 2013). However, these are discussed below, to clarify why they are excluded in this instance.

Table 1. The proportions of the major volcanic rises on Venus (modified from Smrekar and Stofan, 1997)

Volcanic rise	Swell height/km	Swell width-length/km
Rift-dominated		
Beta Regio	2.1	1900–2500
Atla Regio	2.5	1200–1600
Volcano-dominated		
Imdr Regio	1.6	1200–1400
W. Eistla Regio	1.8	2000–2400
Dione Regio	0.5	unknown
Bell Regio	1.2	1100–1400
Corona-dominated		
Themis Regio	1.5	1650–2300
C. Eistla Regio	1.0	1000–1400
E. Eistla Regio	1.0	1600–1800
Terrestrial swells		
Icelandic Rise	2.0	2500
Hawaiian Rise	1.0	1000–2000
Cape Verde Rise	2.2	1800

Two of the three terrestrial rises (Iceland and Hawaii, Hoggard et al., 2020), with the third (Cape Verde, Wilson et al., 2010).

Tables 1 and 2 illustrate the key parameters of each volcano-tectonic structure used in this simple model.

Terrestrial and Venusian large volcanic rises

Those terrestrial hotspots, which lie in ocean basins, are associated with broad swells (Niu, 1997; Sleep 2007; Ramalho et al., 2010; Wilson et al., 2010, 2013; King and Adam, 2014; Hoggard et al., 2020). Dimensions and volumes of these for the Hawaiian and Icelandic Swells are from Hoggard et al. (2020) and the Cape Verde Swell from Wilson et al. (2010).

Terrestrial and Venusian swells, or rises, are clearly comparable in dimension (Smrekar and Stofan, 1997). The swell volume of the 2 km-high Icelandic rise has a volume of 2.6×10^6 km^3, while the 1 km-high Hawaiian rise (swell) has a volume of 1.79×10^6 km^3 (Hoggard et al., 2020). The 2.2 km-high Cape Verde rise (swell), the largest non-plate boundary, magmatic swell on Earth has an approximate volume of 2 million km^3. Terrestrial swells typically have heights in the range of 0.4–2.2 km, with radii that vary from 900 to 1800 km (Monnereau and Cazenave, 1990; Table 1). Swell profiles approximate caps. Using the parameters for the Hawaiian swell, the cap calculation produces a volume of 1.6 million km^3, comparable to the actual value of 1.76 million km^3. Therefore, for the spherical swells, such as the Cape Verde rise, the cap calculation can be used (King and Adam, 2014). However, given the range of terrestrial dimensions produces similar volumes, on the order of 2.0×10^6 km^3 (Monnereau and Cazenave, 1990; Hoggard et al., 2020), we will use this value for Venusian and Terrestrial Rises.

The number of terrestrial swells is approximately three times that seen on Venus (25 versus 9), with the terrestrial majority (20 of 25) on the ocean floor. Swell heights are typically measured below water, and the isostatic loading effect of sea water should

then be removed from the measurement for comparison with Venus. The calculated values are discussed above (Pitman, 1978).

Determination of sea-level changes for differing depths of ocean

The impact of volcano-tectonic structure formation on sea-level depends on the depth of the ocean and the distribution of the structures on the surface of our hypothetical planet. To model this, we used Venusian distributions of highlands, rolling plains and lowland basins (Table 3).

For the purposes of this section of the paper, we assume two depths of ocean (2 and 3 km) and that uplift in one area is offset (compensated) by subsidence in others. Qualitatively, subsidence is hard to determine. On the Earth and Mars, annular subsidence around large volcanic structures is measurable and depends on lithospheric flexure under the weight of the volcanic pile (Kalousová et al., 2010; Klein, 2016; Musiol et al., 2016). In the case of the Hawaiian and other terrestrial swells, downward lithospheric flexure around volcanic edifices is grossly subordinate in magnitude to the effect of the swell and can be discounted. Here, subsidence is given different distributions to illustrate the effect of uplift by the differing structures. For comparison, compensation of regional uplift is assumed to be either global, or in the highland and rolling basins, only. The general formula used to determine the sea-level change with compensation is given by equation (3):

$$A = S.f_u.f_s. \tag{3}$$

Here, A is the actual sea-level change, S is the isostasy-adjusted sea-level changes calculated in Table 4, without compensation; f_u is the fraction of the surface that is submerged, in which uplift occurs; f_s is the fraction of submerged surface in which subsidence occurs. These parameters provide reasonable upper and lower bounds for determining sea-level changes for the tectonic conditions we use. This basic formula is generally applicable although in this instance we use Venusian parameters. Ocean depths <2 km leave structures standing proud of sea-level, reducing their impact, further.

Caveats

While the temporal relationships of the three different classes of volcano-tectonic structures to one-another are reasonably constrained, the relative timescales of their construction are not. Available data suggest emplacement of coronae and novae over 100–200 million year-long (and overlapping) windows (Basilevsky and Head, 1998a, 1998b; Krassilnikov and Head, 2003). Therefore, in this model, changes in sea-level are maximum values that assume (near) simultaneous emplacement. In many cases, the emplacement of coronae is preceded by inflation of large volcanic swells (Smrekar and Stofan, 1997). Secondly, the rate of decay of structures appears relatively slow. Therefore, on Venus (at least) regional tectonism appears to construct structures in waves, leading to geologically-abrupt changes in the corresponding sea-level, were the planet to have oceans.

Table 3 lists the surface area models used for the Venusian landscape. Data are from Magellan (Saunders et al., 1992).

Venusian and terrestrial hypsometric curves

The hypsometric curve defines the area of land within a certain distance from the planet's centre. For the Earth, reference is usually made to sea-level. Figure 4 illustrates the hypsometric curves for the Earth and Venus. Rosenblatt et al. (1994) compare the two curves, using a 2000 m reference point for Venus. The Earth clearly has a bimodal distribution, with ocean floor, continental

Table 2. Determination of the surface area and volume of the three principle large-scale volcano-tectonic features on Venus

Geological feature	Number of features on Venus	Mean radius/km	Mean height/ km	Venusian surface area per feature, (based on mean radius/km^2)	Venusian surface area covered by these features (based on the mean radius)/km^2	Mean Venusian volume per feature/km^3	Total Venusian volume for these features[a]/ km^3
Corona	514	150	0.9	71 000	36 500 000	31 800	1.63×10^7
Nova	64	90	2.0	25 000	1 600 000	25 400	1.63×10^6
Large volcanic rises	9	730–925[b]	1.5	2 200 000	19 400 000	1 610 000	1.45×10^7

Smaller volcanic features, such as domes, shields and lava flows, and areas of rifting are not considered, here. Values in column 4 are to two significant figures; three in the last three. Mean radii of 90 and 150 km were used for novae and for coronae, respectively (Krassilnikov and Head, 2003). Mean heights were also from Krassilnikov and Head (2003) and Basilevsky and Head (1998*a*, 1998*b*). The total volume is based on mean values for area and volume.
[a]The product of the total number of features and their mean volume.
[b]Areas and volumes for large volcanic rises are based on a cap shape, with volume calculated using equation (2). Note that these values are close to the volume of the Hawaiian rise (1.76 × 10^6 km^3) and are within one order of magnitude of the mean terrestrial figure of 2.0 × 10^6 km^3.

Table 3. Surface areas used in the calculation of ocean depth variation, for a Venusian surface

Venusian terrain	Surface area (km^2)
Whole surface	4.6020×10^8
Lowland basin and gently rolling terrain	4.140×10^8
Lowland basins	1.224×10^8

shelf/plains and uplands. For the terrestrial curve, 22.6 million km^2 (15% of the total land area) lies within 100 m of sea-level.

As significant areas of the continental surfaces are within 100 m of current sea-level, relatively small changes in terrestrial ocean depth lead to significant regressions or transgressions. However, for Venusian topography, the effects are more limited.

Marine transgression and albedo

Next, we consider another subtle influence of tectonism in determining biological evolution on planets. The early Earth was an aquaplanet, with limited sub-aerial land (e.g. Rosing *et al.*, 2010; Bindeman *et al.*, 2018). Open ocean has an albedo of 0.06, while barren continental crust, with a granitic composition, has an albedo of 0.3 (Rosing *et al.*, 2010). Plant-covered landscapes, meanwhile, have an albedo closer to 0.21 (Rosing *et al.*, 2010). This implies that during periods of marine transgression, planetary albedo falls, which should, in turn, raise planetary temperatures for a given insolation and cloud cover and composition. For comparison, the Cambrian Sauk Transgression covered 60% of the currently exposed North American craton (Brasier, 1980).

Similarly, the extent of transgression influences the availability of other high albedo landscapes, such as desserts or ice caps. In general, such landscapes must be less common on planets where the ocean cover is more extensive. For the Earth, a rise of 100 m drowns 22.6 million km^2, or 16%, of the sub-aerial surface, reducing the albedo of the affected area from approximately 0.3 for a granitic desert to 0.06 for open ocean in the affected area (Rosing *et al.*, 2010). Likewise, for a vegetated landscape, the albedo is approximately 0.21 (Rosing *et al.*, 2010).

Planetary albedo is estimated as follows using the proportion of the surface that has one albedo (e.g. ocean) or another.

$$\alpha_{\mathrm{P}} = \frac{(x_A.f_A) + (x_B.f_B)}{100}, \tag{4}$$

where x_A is the albedo of area A; x_B is the albedo of area B and f_A and f_B are the relative fraction of surface with these values of albedo, respectively (shown here as percentages, but can be as a decimal fraction). As before, changes in cloud cover are ignored.

Simple scaling arguments can be used to determine the change in surface albedo, thereby, ignoring the effects of any changes to cloud cover. For illustrative purposes, a reduction in land area, associated with a 100 m sea-level rise, global albedo falls from 0.13 to 0.12.

The following expression is then used to determine the change in global temperature.

$$T = \sqrt[4]{\frac{A_{\mathrm{abs}}}{A_{\mathrm{rad}}} \frac{L(1 - \alpha)}{4\pi\sigma\varepsilon D^2}}, \tag{5}$$

where α is the albedo, and with realistic values of emissivity, ε, at 0.96, Earth orbital radius, D at 1.5×10^{11} m, Stefan's constant 5.67×10^{-8} watt per meter squared, per Kelvin to the fourth (W m^{-2} K^{-4}). L is the current solar luminosity, 3.828×10^{26} W. The ratio of the absorbing area (A_{abs}) versus radiating area (A_{rad}) for the Earth may be approximated as 0.25 for its current rotation rate.

Species–area relationships

The SAR can be used to estimate the change in the number of microbial, marine or terrestrial (land) species with a change in land area (Lomolino, 2000; Gray, 2001; Azovsky, 2002). This precise mathematical relationship between species richness and land-area varies with the ecosystem (Gray, 2001; Gerstner *et al.*, 2014).

$$S = CA^z, \tag{6}$$

which gives a linear relationship with logarithmic axes, as follows.

$$\log_{10} S = \log_{10} C + z \log_{10} A. \tag{7}$$

For shallow marine environments, C has the value of 1.7 and z has the value of 0.05 (Gray, 2001, for illustrative purposes only).

Results

Tectonism and ocean depth

Table 4 illustrates the effect of coronae and novae on ocean depth on Venus, with assumptions regarding the area of ocean on a

Table 4. A comparison of the net gain in sea-level for the Cretaceous geological events from Müller *et al.* and approximate equivalent changes for a Venusian tectonic regime

Geological process	Planet	Volume of structure (Table 2)/km³	Change in ocean depth/ m	Adjustment for isostatic loading/m	Notes
Large Igneous Provinces (LIPs)	Earth	–	100		From Müller *et al.* (2008)
Formation of young, buoyant ocean ridges	Earth	–	70		From Müller *et al.* (2008)*
Seamounts	Earth	–	11		From Conrad (2013)
Coronae	Earth[a]	1.63×10^7	31.7	22.2	The weight of oceans reduces the height of the structures by 30% relative to those observed on Venus
	Venus[b]		39.4	27.6	
	Venus[c]		133	93.1	
Novae	Earth[a]	1.63×10^6	2.42	1.69	
	Venus[b]		2.95	2.07	
	Venus[c]		9.98	6.98	
Large volcanic rises	Earth[a]	1.45×10^7	40.0	28.0	
	Venus[b]		35.0	24.5	
	Venus[c]		118	82.6	

Change in Venusian volume are modelled as simple displacements and do not include the gravitational effects of adding mass to particular regions, nor any effect of subsidence or sedimentation. The Venus models have the following surface areas applied: a – Earth Current Area of Oceans for comparison; b –all coronae and novae in lowlands and rolling terrain; c – lowlands, only, ocean with all coronae and novae in the lowlands. *The range on the LIP and young oceanic crust effect on sea-level is from +90 to +265 m (Müller *et al.*, 2008).
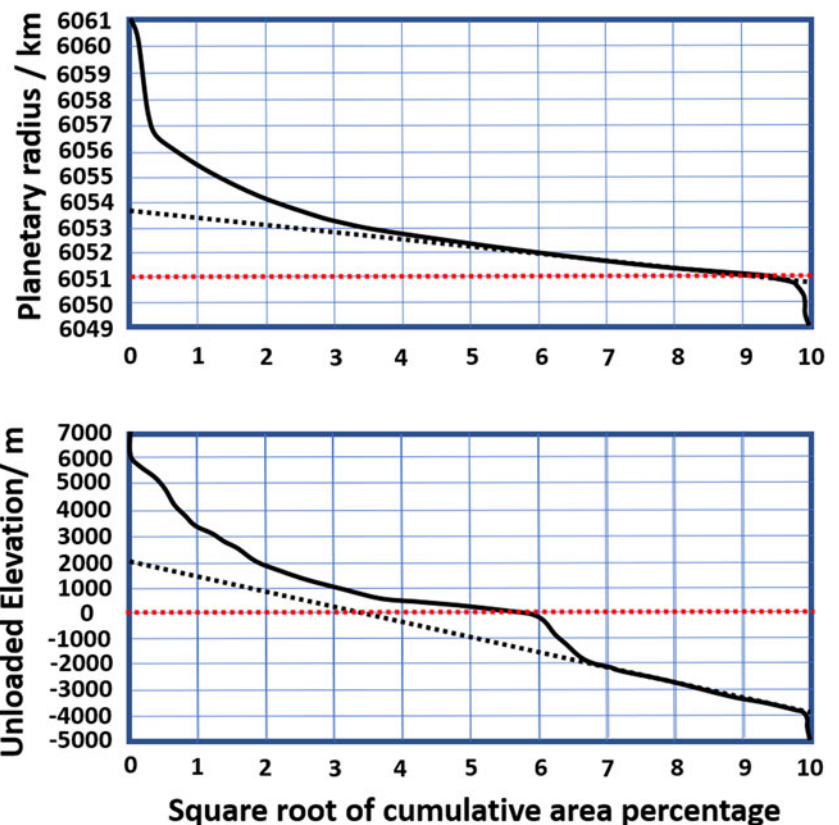

Fig. 4. Global cumulative hypsometric curves for Venus (top) and the Earth (bottom). Dashed black lines are the best linear regression fits. Modified from Rosenblatt *et al.* (1994). Dashed red lines mark nominal sea-level on Earth, while heights at Venus are referenced to a sphere of radius 6051.0 km, corresponding to the mean radius of the planet.

Venus-like planet, which lacked plate tectonics, but had Venusian-style regional tectonism. Table 4 includes the effects of ocean-ridge systems and oceanic LIPs on ocean depth from Müller *et al.* (2008) and Conrad (2013) for comparison.

Coronae, novae and large volcanic rises are thought to be the surface manifestations of the arrival of plume heads of varying dimensions, at the base of the Venusian lithosphere (Basilevsky and Head, 1998*a*, 1998*b*; Krassilnikov and Head, 2003).

Terrestrial rises and LIPs are, therefore, analogous (Müller *et al.*, 2008; Niu *et al.*, 2017). However, given the geospatial relationship of some coronae to large volcanic rises, the manner in which their plumes impinge the lithosphere is more complex than terrestrial structures. For all geospatial scenarios, the effect of novae sea-level is limited. However, the effect of both the large volcanic rises and the coronae on Venusian sea-level is comparable to that of young ocean ridges and LIPs on terrestrial sea-level. From our analysis, the volume change to oceans caused by novae would be similar to that caused by terrestrial seamounts (on the order of 10^0–10^1 m, Conrad, 2013).

Assuming near-constant mantle volume, swells in one area must be off-set by subsidence in others. Referring to this as compensation, Tables 5 and 6 illustrate the effect of subsidence for differing scenarios of uplift and subsidence distributions and ocean depths.

Using Venusian parameters, 10% of the surface is highland and not drowned with either two or three km depth of ocean; 63% is gently rolling plains of intermediate height (2–3 km above the plain) and 27% is lowland basin, <2 km above the plain (Rosenblatt *et al.*, 1994). Table 5 illustrates the impact of compensating subsidence for an uplift in the lowland basins and rolling uplands only, but with compensating subsidence in the highlands and rolling plains, or across the whole surface.

Next, we look at the same parameters of ocean depth and distribution of compensation, but restrict the uplift to the lowland basins. In this scenario, the change in the relative distribution of uplift to subsidence has a significant effect on sea-level change. With a shallow ocean (<2 km), the features are submerged but compensation occurs over the remaining 73.6% of the planet's surface, generating a rise in sea-level equivalent to that determined in Table 6. However, once the sea-level is increased and drowns the rolling plains, compensation by subsidence once again largely offsets rises caused by inflation of the tectonic structures.

Therefore, we conclude that the effect of regional tectonism is strongly dependent on ocean depth and where uplift is compensated. Larger areas of highland will produce proportionately greater changes in ocean depth, where uplift is dominated in the basins.

Figure 5 shows the relative impact of different Venusian volcano-tectonic structures on sea-level on hypothetical planets of varying ocean area, with the assumption that all of the features will fall into the ocean basins and there is no offsetting subsidence in these basins. Again, the depth changes are adjusted for isostatic loading.

Overall, the effect of the larger Venusian tectonic structures on sea-level rise is within an order of magnitude of that caused by the formation of new ocean basins, with buoyant ridges, but only where the oceans are shallow and uplift is compensated by subsidence outside of the basin. Applied to the Venusian hypsometric curve, less area would be flooded than if the Earth's land distribution was used. However, as the terrestrial curve is a product of both the presence of continental crust and its erosion and deposition relative to sea-level, the difference is academic. Here, we would assume the presence of oceans will cause the continental crust to assume the broadly flat aspect in relation to the sea-level. The key factor is the volume of continental crust, which is limited in extent on Venus (perhaps 10%, Hashimoto *et al.*, 2008) but abundant on Earth (40% of the surface). Therefore, while a 100 m sea-level rise on Earth leads to extensive transgression, covering over 20 million km^2, a similar rise on a planet with Venusian hypsometric curve will cover <10% of this area.

Importantly, while we have a good understanding of the temporal scale of tectonic processes on Earth, we do not have a similar grasp of structure formation and decay on Venus. However, future missions to Venus may clarify these temporal relationships. From here, we can then consider the rate of change of sea-level on planets that may be comparable to Venus, in terms of tectonic style.

In conclusion, while Venusian-style tectonism can produce comparable sea-level changes to those produced by plate tectonics, the hypsometric curve is critical in determining the geographical extent of the resulting transgression. For the terrestrial bimodal hypsometric curve, where there is the formation of coronae or large volcanic rises to substitute for plate tectonics, there would be significant transgressions covering land areas comparable to those seen in the Phanerozoic. Therefore, the Venusian mode of tectonism could drive the biological diversification and mass extinction seen on Earth (Brasier, 1980, 1982; Banerjee *et al.*, 1997; Banerjee and Mazumdar, 1999; Squire *et al.*, 2006; Peters and Gaines, 2012; Landing and Kouchinsky, 2016; Clemmensen *et al.*, 2017; Karlstrom *et al.*, 2018; Latif *et al.*, 2018; Wei *et al.*, 2018; Paterson *et al.*, 2019). However, while this is true, the Venusian mode of regional tectonism is not associated with a comparable hypsometric curve. Therefore, the transgressive effect would be more limited if the planet lacked similarly extensive areas of continental crust as the Earth.

Marine transgressions and planetary albedo

Next, we consider whether a realistic marine transgression will change the albedo sufficiently to alter the overall temperature of the planet. We take the Earth's hypsometric curve and land area, then raise sea-level by 100 m. The early Earth was an aquaplanet, with limited sub-aerial land (Flament *et al.*, 2008; Rosing *et al.*, 2010; Bindeman, *et al.*, 2018). The albedo of open ocean is considerably lower than that of continental crust (0.06 versus 0.30). Applying a transgression of 100 m to the Earth's current hypsometric curve will result in an inundation of 22 million km^2 of land (14.7% of the total land area). From simple surface area relationships, and ignoring any changes in cloud cover, planetary albedo is reduced from 0.13 to 0.12 during the accompanying transgression on vegetation-free land.

Likewise, for a planet with a terrestrial land area of 149 million km^2, terrestrial hypsometric curve and plant-coverage, a 100 m sea-level rise reduces the land area to 127.5 million km^2. The corresponding albedo is 0.0975. For the equivalent vegetated planet, but without the transgression, the albedo will be 0.1035. Ignoring variation in cloud-cover, the difference in albedo is 0.006, which changes the effective surface temperature by 0.28 K. Table 7 summarizes these results for surface albedo and temperature.

Therefore, we conclude that a 100 m sea-level rise and accompanying transgression on the terrestrial hypsometric curve has a small but measurable effect on global temperature. The effect of transgressions is greatest for planets with greater areas of more reflective non-vegetated land.

Table 8 shows the area of land drowned during terrestrial Phanerozoic transgressions, for comparison. The Cambrian (Sauk) transgressions were more extensive than would be expected today because the hypsometric curve was different. The Cambrian terrain was much closer to sea-level, probably as a result of late Proterozoic glaciation (Keller *et al.*, 2019). Therefore, sea-level rises, on the order of 90 m inundated far larger areas of the continent than would be seen today.

Table 5. Effect of uplift in the lowland basins and rolling plains, only, but with off-setting subsidence in the rolling plains and highlands versus the whole surface

Ocean depth/km	Change of ocean depth with distribution of subsidence/m					
	Compensation in highland and rolling plains only			Global compensation		
	Novae	Coronae	Rises	Novae	Coronae	Rises
≤2	0.41	5.60	5.04	0.37	5.10	4.50
3	0.20	2.70	2.40	0.20	2.70	2.40

The ocean depth has a relatively small effect as the distribution of uplift and subsidence relative to sea-level is slight.

Table 6. The effect of uplift, exclusively in the lowland basins, where off-setting subsidence is restricted to other areas of the planet; and for two depths of ocean

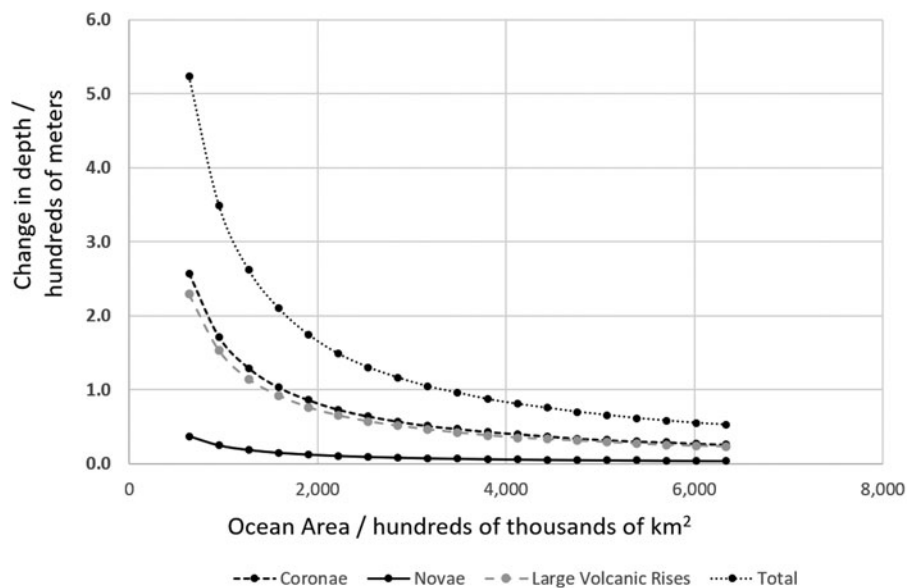| Ocean depth/km Feature class	Change of ocean depth with distribution of subsidence/m					
	Highland and rolling plains only			Even distribution		
	Novae	Coronae	Rises	Novae	Coronae	Rises
≤2	6.98	93.1	82.6	5.15	68.5	60.8
3	0.69	9.31	8.26	0.69	9.31	8.26

Fig. 5. Relative change in ocean depth for various volcano-tectonic features and varying ocean area.

Table 9 illustrates the potential change in surface temperature for a given albedo and ignoring the effects of cloud cover.

We show that terrestrial transgressions will alter surface temperature, by altering surface albedo, in the absence of changes to cloud cover. Therefore, aside from altering the distribution of habitats, transgressions can also alter the surface temperature. The mode of tectonism, therefore, has evolutionary impacts that extend beyond altering, eliminating or creating habitats.

Marine transgressions and evolutionary diversification

In this section, we review the likely impacts of sea-level change on biodiversity and evolution. We consider, first, the impact of plate tectonics, then Venusian tectonics. Clearly, we cannot anticipate the path that the evolution of life will take on an alien world, other than to specify, by definition, evolution is an increase in the complexity of all life. Now, specifically, this increase in complexity is manifest as an increase in the complexity of the information present, following the rules of information entropy. We can illustrate the increase, or change, in complexity through the SAR (Lomolino, 2000; Gray, 2001; Azovsky, 2002; Neigel, 2003).

If we apply terrestrial marine values of C as 1.7 and z as 0.05, then for every increase of one million km², the number of marine species would increase by 52. While SARs are unique to each class of organism in each environment, the principle applies to all terrestrial life, whether microbial or multicellular (Lomolino, 2000). Therefore, one expects that marine transgression or regression must, by definition, increase or decrease species diversity. Initial flooding would be expected to eliminate subaerial habitats, while creating novel shallow marine habitats, and *vice versa*.

Table 7. Changes in surface albedo and corresponding temperature for three scenarios relative to a planet with terrestrial land area (149 million km^2 and ocean area 361.9 million km^2) and no vegetation

Geographical change relative to current land area	Surface albedo	Relative temperature change/K
Non-vegetated surface, current land area	0.130	/
Vegetated surface, current land area	0.1035	0.43
Non-vegetated, 100 m sea-level rise	0.120	0.28
Vegetated surface, 100 m sea-level rise	0.0975	0.40

The effect of cloud-cover is ignored.

Table 8. Changes in surface albedo for the six Phanerozoic transgressions

| Transgression | Geological era | Estimated transgressed surface area/km^2 | | | | Relative change in surface albedo |
		North America	South America	Africa	Total	
Sauk	Cambrian	12 000 000	1 400 000	9 000 000	23 000 000	*0.01
Tippecanoe	Upper Ordovician	10 250 000	4 300 000	9 000 000	23 500 000	0.0065
Kaskaskia	Upper Devonian	11 000 000	4 400 000	7 400 000	22 800 000	0.0065
Absaroka	Permian	11 500 000	6 200 000	17 900 000	35 600 000	0.0095
Zuni	Cretaceous	16 000 000	14 200 000	26 600 000	56 800 000	0.0165
Tejas	Eocene	15 000 000	15 800 000	24 400 000	55 200 000	0.0155

For the Cambrian (Sauk) transgressions, the value for land albedo is that of barren granitic desert (0.3), while for later transgressions, surface albedo is set at 0.21 for vegetated landscape. Ocean albedo is set at 0.06. Comparison is made for contemporaneous land area (29%).* The value for the Sauk transgression is based on a change in area from granitic desert to ocean; while the latter ones are from vegetated landscapes to ocean.

Table 9. Changes to surface temperature for a given surface albedo and ignoring the effects of clouds

Transgression	Relative change in surface albedo	Relative change in temperature/K
Sauk	*0.01	0.32
Tippecanoe	0.0065	0.28
Kaskaskia	0.0065	0.28
Absaroka	0.0095	0.31
Zuni	0.0165	0.36
Tejas	0.0155	0.35

In this analysis, transgressions consistently drive rises approximating 0.3 K, relative to current land area (149 million km^2) with vegetated or *non-vegetated landscapes and land albedo values equivalent to those in Table 6.

The precise impact of regression or regression depends on the hypsometric curve for the planet in question. Planets with strongly bimodal distributions, where much of the land lies close to sea-level, should expect strong changes in species diversity with changes in sea-level. Planets with steeper hypsometric curves will show proportionately lower changes in species diversity as transgression or regression will be more limited in extent.

Discussion

In this paper, we discuss the impact of Venusian-style tectonism on ocean depth, given various scenarios for ocean area. We then consider the knock-on effects of ocean transgression on any biosphere. In particular, we ask how marine transgressions might affect the availability of habitats, nutrients and, finally, climate.

While we have used relatively simple models to determine the volume of each structure, volume calculations for the large volcanic rises come close to the values determined by other means, thereby validating the overall approach (King and Adam, 2014; Hoggard *et al.*, 2020). We can conclude that planets with Venusian-style regional tectonism can experience comparable transgression events to those associated with terrestrial tectonism, whether this is hot spot-related or plate-tectonics. However, the magnitude of sea-level rise is dependent on the location of the event(s) that give rise to it and the location of any associated subsidence. Applied to our model planet, Venus, with its distribution of highland, upland and lowland crust, then only in the extreme scenario, where we have relatively shallow seas and uplift confined to the basins, do we see large transgressions comparable in magnitude to those seen on Earth. In most other scenarios that we tested, sea-level changes are far more modest, on the order of a few metres or less. However, we note that even the modest scale of the rises that are seen in these models would still have a notable impact on coastal erosion and sea-level advance. The relationship between sea-level rise and erosion (Bruun equation 1) would cause a retreat two orders of magnitude greater than the observed rise, potentially releasing considerable additional debris and nutrients to any coastal environment (Zhang, 1998; Zhang *et al.*, 2004).

The precise magnitude of any transgression is also dependent on the planet's hypsometric curve. For the Earth, tens of millions of square kilometres of land lie within 200 m of current sea-level. Modest rises, therefore, bring about significant changes to the location of coastlines. On Venus, which lacks oceans, the

hypsometric curve appears to principally relate to the location of volcano-tectonic structures, rather than to sedimentation or the presence of widespread sialic crust (Hashimoto *et al.*, 2008). Other worlds could be envisaged that have a greater prevalence of sialic crust but regional tectonism – as appears the case in the terrestrial Archean era (Rozel *et al.*, 2017). Such worlds may have hypsometric curves that are a closer match to the current Earth than barren Venus.

Next, we examined the effect of transgression on planetary albedo, using the terrestrial transgressions as examples. As one might expect from changing the land-sea distribution, transgression lowers global albedo and, therefore, can raise planetary temperature; precisely the mechanism identified by Rosing *et al.* (2010) to keep the early Earth warm. In this instance, we are looking at more modest changes in sea-level and more modest changes in temperature; however, the effect may still yield biological changes. Moreover, changes to temperature would be expected to generate further change through positive and negative feedback mechanisms. For example, increases in temperature increase the rate of respiration of any extant microorganisms (Heimann and Reichstein, 2008). Increases in respiration lead to amplification in carbon dioxide production and hence, further rises in the proportion of greenhouse gases. For example, Scheffer *et al.* (2006) suggest that feedback will promote a 15–78% increase in temperature on century timescales. Secondly, loss of land surface and rises in temperature will reduce any ice cover (Pistone *et al.*, 2019). This process will also lead to a reduction in albedo and further rises in temperature. A final and critical feedback concerns the well-known carbonate-silicate cycle (Walker *et al.*, 1981). Increases in the erosion of silicate bedrock increase carbon sequestration on millennial and longer timescales. The rate of this process increases with higher temperature. Therefore, when considering the impact of lower albedo on planetary temperature, one must also consider how increases in the rate of erosion of non-transgressed land will affect the longer-term changes in the temperature of the planet.

Marine photosynthetic organisms are known to affect cloud formation (Rosing *et al.*, 2010). Enhanced erosion at the wave-cut margins (razoring), which is associated with transgression, should lead to blooms of microorganisms in the oceans, as marine transgression liberates nutrients. On Earth, plants and algae produce the majority of cloud-condensation-nuclei (CCNs, Rosing *et al.*, 2010). Blooms of algae might be expected consequent to marine transgression, as ocean waters erode material from the receding continental margins and liberate nutrients. Conversely, there is a significant contribution to CCN from feldspar particles, which initiate the formation of ice crystals (Kiselev *et al.*, 2017). Reduction in the availability of land would reduce the abundance of feldspar aerosols, thereby reducing cloud formation, particularly on planets with limited biospheres. The uncertainty in the confounding effects of wind versus wave-driven erosion on the availability of different CCN means that we did not pursue cloud-driven albedo changes in this work but seems a fertile area for further work.

Similarly, while the Earth likely, currently, experiences a net regassing of the mantle (Korenaga *et al.*, 2017), planets lacking plate tectonics will progressively degas at a rate dependent on their mass, internal radiogenic budget and the mode of mantle convection (Schaefer and Sasselov, 2015). Without a means to lose surface water, either to space or by tectonism to the mantle, ocean levels will increase, in a declining upward trend, leading to progressive drowning of surface features.

What are the likely impacts on the evolution of life on planets that experience Venus-like tectonism? If we ignore the risk of complete drowning of the surface through progressive degassing or sedimentation, variations in tectonic rate will lead to transgressions and regressions in a manner similar to those seen on Earth but of lower magnitude. To quantify some of the likely effects, we use SAR as a proxy for species distribution with land (or shallow marine) areas. Focussing on transgression and values for marine species taken from Gray (2001), we can readily show that increases in shallow marine environments will also increase species richness (the variety of species present). We also note that allopatric speciation (the formation of new species following geographical separation) is facilitated by the formation of new landscapes (Heenan and McGlone, 2013; Rahbek *et al.*, 2019). During marine transgression, land habitats are eliminated and marine habitats are created. For planets with predominantly marine biotas, such as the terrestrial Cambrian and Ordovician eras, the creation of an abundance of habitats is associated with strong evolutionary diversification. The loss of many of these habitats in the late Ordovician is associated with mass extinction (Barash, 2014).

Therefore, if marine transgression was a trigger (or one of a few triggers) for the Cambrian Explosion (Peters and Gaines, 2012) and for various extinction events (Solé *et al.*, 2003; Squire *et al.*, 2006; Bond and Wignall, 2008; Vodráqková *et al.*, 2013; Barash, 2014; Brocke *et al.*, 2015; López-Villalta, 2016; Percival *et al.*, 2018), then we can anticipate Venusian-style regional tectonism can drive similar evolutionary processes on worlds that experience these kinds of tectonic events. The magnitude of the transgression depends on the location of any uplift and associated subsidence; but also, on the depth of any oceans.

That planets that lack plate tectonics may progressively drown must also be considered. Degassing could be prompt, so that the majority of available water is released early, with little variation later on. To such worlds, volcano-tectonic activity might then build subaerial structures, if water depths are not extreme. Schaefer and Sasselov (2015) consider different planetary models with different rates of degassing. The largest worlds in their models may take a few billion years to degas, while others show prompt degassing. Regassing was relatively fast for some of their model worlds – however, these models were assumed to have plate tectonics. Rapid growth of continental crust, which may choke off plate tectonics, is rarely considered (Lenardic *et al.*, 2005). Determining whether planets will host plate tectonics for realistic masses and rates of continental growth awaits further modelling. Planets that initially have hot stagnant lids may have regional tectonism, like Venus, but grow continental crust so quickly that the surface becomes too buoyant for subduction to occur (Kite *et al.*, 2009).

Ultimately, the impact of changes to ocean depth on evolutionary progression will clearly be context-related. If one considers the Earth, then on a planet that was otherwise rather barren in the Neoproterozoic, marine transgression may have eliminated (or created) prokaryotic niches, but little else until late in the era. More fundamentally, 3.0–2.7 billion years ago, most of the Earth's continental crust was submerged (Flament *et al.*, 2008; Bindeman *et al.*, 2018; Cawood *et al.*, 2018) but the advent of modern plate tectonics brought about (or as it is least associated with) the emergence of 90% of the current land surface. Shortly, thereafter there is a succession of glaciations, which one would expect following an increase in global albedo that would be associated with the emergence of land (a change in albedo from 0.06

to 0.3, Rosing *et al.*, 2010). Moreover, during the period from 2.7 to 2.5 Gya, most of the large continental bodies are thought to have been assembled in the Kenorland supercontinent (Yakubchuk, 2019). The formation of the supercontinent would be associated with uplift and enhanced weathering, and a decrease in sea-level. The subsequent dispersion of Kenorland after 2.5 Gy would be accompanied by marine transgression as new, buoyant oceanic lithosphere raised the level of the ocean floor. It is noteworthy, then that the GOE occurs in the time-frame associated with marine transgression and the formation of new, shallow, ocean margins (Philippot *et al.*, 2018).

In the Cambrian and early Ordovician, transgressions are associated with great biological diversification. Conversely, during the Devonian, transgressions are linked to global and regional extinction events. In turn, extinction events lead to the opening of new niches for life, promoting innovation in the longer term. Likewise, the biological innovations of the Cambrian that led to us follow the wholesale extinction of the Ediacaran lineages. Transgressions may thus be as much a razor for life as they are for the bedrock, over which they sweep.

In this regard, Rosing *et al.* (2010) identify a final factor of relevance to the long-term survival of life on a planet. Consider a world lying near the inner edge of the habitable zone, where global plate tectonics does not operate. Here, degassing continues and the surface progressively drowns. While there are immediate losses of biological niche spaces on land (and the growth of marine niche spaces), there will be a decrease in planetary albedo that is associated with the loss of continental surface. Therefore, in the longer term, progressive transgression could warm the planet through the reduction in albedo, so that it experiences a thermal runaway. Additional feedbacks clearly need consideration.

There are a considerable number of variables that can influence ocean depth on planets where regional tectonic processes dominate. As a first step, this paper examines a few of these variables, using Venusian tectonism as a model starting point. However, we hope that it is clear that there are several other factors that should be considered if we are then to extrapolate to any impact of tectonic style on habitability and the evolvable potential of any life that emerges.

References

Azovsky AI (2002) Size-dependent species-area relationships in benthos: is the world more diverse for microbes? *Ecography* **25**, 273–282.

Banerjee DM and Mazumdar A (1999) On the late Neoproterozoic-early Cambrian transition events in parts of east Gondwanaland. *Gondwana Research* **2**, 199–211.

Banerjee DM, Schidlowski M, Siebert F and Brasier MD (1997) Geochemical changes across the Proterozoic–Cambrian transition in the Durmala phosphorite mine section, Mussoorie Hills, Garhwal Himalaya, India. *Palaeogeography, Palaeoclimatology, Palaeoecology* **132**, 183–194.

Barash MS (2014) Mass extinction of the marine biota at the Ordovician–Silurian transition due to environmental changes. *Oceanology* **54**, 780–787.

Basilevsky AT and Head III JW (1998a) The geologic history of Venus: a stratigraphic view. *Journal of Geophysical Research* **103**, 8531–8544.

Basilevsky AT and Head JW (1998b) Onset time and duration of corona activity on Venus: stratigraphy and history from photogeologic study of stereo images. *Earth, Moon and Planets* **76**, 67–115.

Becker RT, Königshof P and Brett CE (2016) Devonian climate, sea level and evolutionary events. *Geological Society, London, Special Publications* **423**, 123–169.

Bindeman IN, Zakharov DO, Palandri J, Greber ND, Dauphas N, Retallack GJ, Hofmann A, Lackey JS and Bekker A (2018) Rapid emergence of subaerial landmasses and onset of a modern hydrologic cycle 2.5 billion years ago. *Nature* **557**, 545–548.

Bolmont E, Selsis F, Owen JE, Ribas I, Raymond SN, Leconte J and Gillon M (2017) Water loss from terrestrial planets orbiting ultracool dwarfs: implications for the planets of TRAPPIST-1. *Monthly Notices of the Royal Astronomical Society* **464**, 3728–3741.

Bond DPG and Wignall PB (2008) The role of sea-level change and marine anoxia in the Frasnian–Famennian (Late Devonian) mass extinction. *Palaeogeography, Palaeoclimatology, Palaeoecology* **263**, 107–118.

Brasier MD (1980) The Lower Cambrian transgression and glauconite-phosphate facies in western Europe. *Journal of the Geological Society* **137**, 695–703.

Brasier MD (1982) Sea-level changes, facies changes and the late Precambrian – early Cambrian evolutionary explosion. *Precambrian Research* **17**, 105–123.

Brocke R, Fatka O, Lindemann RH, Schindler E and Ver Straeten CA (2015) Palynology, dacryoconarids and the lower Eifelian (Middle Devonian) Basal Choteč Event: case studies from the Prague and Appalachian basins. *Geological Society, London, Special Publications* **423**, 123–169.

Budd GE and Jackson ISC (2016) Ecological innovations in the Cambrian and the origins of the crown group phyla. *Philosophical Transactions of the Royal Society B* **371**, 20150287.

Carr MH and Head JW (2015) Martian surface/near-surface water inventory: sources, sinks, and changes with time. *Geophysical Research Letters* **42**, 1–7.

Cawood PA, McCausland PJA and Dunning GR (2001) Opening Iapetus: constraints from the Laurentian margin in Newfoundland. *Geological Society of America Bulletin* **113**, 443–453.

Cawood PA, Hawkesworth CJ, Pisarevsky SA, Dhuime B, Capitanio FA and Nebel O (2018) Geological archive of the onset of plate tectonics. *Philosophical Transactions of the Royal Society A* **376**, 20170405.

Clemmensen LB, Glad AC, Gunver K and Pedersen GK (2017) Early Cambrian wave-formed shoreline deposits: the Hardeberga Formation, Bornholm, Denmark. *International Journal of Earth Sciences (Geol Rundsch)* **106**, 1889–1903.

Coffin MF and Eldholm O (1994) Large igneous provinces: crustal structure, dimensions, and external consequences. *Reviews of Geophysics* **32**, 1–36.

Colmenar J and Rasmussen CMØ (2017) A Gondwanan perspective on the ordovician radiation constrains its temporal duration and suggests first wave of speciation, fuelled by Cambrian clades. *Lethaia* **51**(2), 286–295.

Conrad CP (2013) The solid Earth's influence on sea level. *Geological Society of America Bulletin* **125**, 1027–1052.

Dohm JM and Maruyama S (2015) Habitable trinity. *Geoscience Frontiers* **6**, 95–101.

Domeier M (2016) A plate tectonic scenario for the Iapetus and Rheic oceans. *Gondwana Research* **36**, 275–295.

Duran S, Coulthard TJ and Baynes ERC (2019) Knickpoints in Martian channels indicate past ocean levels. *Nature Scientific Reports* **9**, 15153.

Flament N, Coltice N and Rey PF (2008) A case for late-Archaean continental emergence from thermal evolution models and hypsometry. *Earth and Planetary Science Letters* **275**, 326–336.

Fox D (2016) What sparked the Cambrian Explosion? *Nature* **530**, 268–270.

Gerstner K, Dormann CF, Vaclavík T, Kreft H and Seppelt R (2014) Accounting for geographical variation in species–area relationships improves the prediction of plant species richness at the global scale. *Journal of Biogeography* **41**, 261–273.

Gladczenko TP, Coffin MF and Eldholm O (1997) Crustal structure of the Ontong Java Plateau: modeling of new gravity and existing seismic data. *Journal of Geophysical Research* **102**, 22711–22729.

Gray JS (2001) Marine diversity: the paradigms in patterns of species richness examined. *Scientia Marina* **65**, 41–56.

Grazhdankin D (2004) Patterns of distribution in the Ediacaran biotas: facies versus biogeography and evolution. *Paleobiology* **30**, 203–221.

Grindrod PM and Trudi Hoogenboom T (2006) Venus: the corona conundrum. *Astronomy and Geophysics*, **47**, 3.16–3.21.

Hashimoto GL, Roos-Serote M, Sugita S, Gilmore MS, Kamp LW, Carlson RW and Baines KH (2008) Felsic highland crust on Venus suggested by Galileo Near-Infrared Mapping Spectrometer data. *Journal of Geophysical Research* **113**, E00B24.

Heenan PB and McGlone MS (2013) Evolution of New Zealand alpine and open-habitat plant species during the late Cenozoic. *New Zealand Journal of Ecology* **37**, 105–113.

Heimann M and Reichstein M (2008) Terrestrial ecosystem carbon dynamics and climate feedbacks. *Nature* **451**, 289–292.

Hodych JP and Cox RA (2007) Ediacaran U–Pb zircon dates for the Lac Matapédia and Mt. St.-Anselme basalts of the Quebec Appalachians: support for a long-lived mantle plume during the rifting phase of Iapetus opening. *Canadian Journal of Earth Sciences* **44**, 565–581.

Hoffman PF, MacDonald FA and Halverson GP (2011) Chapter 5 – chemical sediments associated with Neoproterozoic glaciation: iron formation, cap carbonate, barite and phosphorite. In Arnaud E, Halverson GP and Shields-Zhou G (eds). *The Geological Record of Neoproterozoic Glaciations*. London: The Geological Society of London, pp. 0435–4052. doi: 10.1144/M36.5.

Hoggard MJ, Parnell-Turnerc R and Whited N (2020) Hotspots and mantle plumes revisited: towards reconciling the mantle heat transfer discrepancy. *Earth and Planetary Science Letters* **542**, 116317.

Kalousová K, Souček O and Čadek O (2010) Global model of elastic lithosphere thickness on Mars. *EPSC Abstracts* **5**, EPSC2010-608.

Karlstrom K, Hagadorn J, Gehrels G, Matthews W, Schmitz M, Madronich L, Mulder J, Pecha M, Giesler D and Crossey L (2018) Cambrian Sauk transgression in the Grand Canyon region redefined by detrital zircons. *Nature Geoscience* **11**, 438–443.

Kasting JF and Holm NG (1992) What determines the volume of the oceans? *Earth and Planetary Science Letters* **109**, 507–515.

Keller CB, Husson JM, Mitchell RN, Bottke WF, Gernon TM, Boehnke P, Bell EA, Swanson-Hysell NL and Peters SE (2019) Neoproterozoic glacial origin of the Great Unconformity. *Proceedings of the National Academy of Sciences* **116**, 1136–1145.

Keresztúri Á, Hagen TH, Bleamaster LF and Hargitai H (2015) Corona (Venus). In Hargitai H and Keresztúri Á (eds). *Encyclopedia of Planetary Landforms*. New York, NY: Springer.https://doi.org/10.1007/978-1-4614-3134-3_439.

King SD and Adam C (2014) Hotspot swells revisited. *Physics of the Earth and Planetary Interiors* **235**, 66–83.

Kirschner JP, Kominz MA and Mwakanyamale KE (2010) Quantifying extension of passive margins: implications for sea level change. *Tectonics* **29**, TC4006.

Kiselev A, Bachmann F, Pedevilla P, Cox SJ, Michaelides A, Gerthsen D and Leisner T (2017) Active sites in heterogeneous ice nucleation – the example of K-rich feldspars. *Science (New York, N.Y.)* **355**, 367–371.

Kite ES, Manga M and Gaidos E (2009) Geodynamics and rate of volcanism on massive Earth-like planets. *The Astrophysical Journal* **700**, 1732–1749.

Klein FW (2016) Lithospheric flexure under the Hawaiian volcanic load: internal stresses and a broken plate revealed by earthquakes. *Journal of Geophysical Research: Solid Earth* **121**, 2400–2428.

Korenaga J (2011) Thermal evolution with a hydrating mantle and the initiation of plate tectonics in the early Earth. *Journal of Geophysical Research* **116**, B12403.

Korenaga J, Planavsky NJ and Evans David AD (2017) Global water cycle and the coevolution of the Earth's interior and surface environment. *Philosophical Transactions of the Royal Society A* **375**, 20150393.

Krassilnikov AS and Head JW (2003) Novae on Venus: geology, classification, and evolution. *Journal of Geophysical Research* **108**, 5108.

Kurokawa H, Foriel J, Laneuville M, Houser C and Usui T (2018) Subduction and atmospheric escape of Earth's seawater constrained by hydrogen isotopes. *Earth and Planetary Science Letters* **497**, 149–160.

Landing E and Kouchinsky A (2016) Correlation of the Cambrian evolutionary radiation: geochronology, evolutionary stasis of earliest Cambrian (Terreneuvian) small shelly fossil (SSF) taxa, and chronostratigraphic significance. *Geological Magazine* **153**, 750–756.

Latif K, Xiao E, Riaz M, Wang L, Khan MY, Hussein AA and Khan MU (2018) Sequence stratigraphy, sea-level changes and depositional systems

in the Cambrian of the North China Platform: a case study of Kouquan section, Shanxi Province. China. *Journal of Himalayan Earth Sciences* **51**, 1–16.

Lee MYS, Soubrier J and Edgecombe GD (2013) Rates of phenotypic and genomic evolution during the Cambrian explosion. *Current Biology* **23**, 1889–1895.

Lenardic A, Moresi LN, Jellinekc AM and Manga M (2005) Continental insulation, mantle cooling, and the surface area of oceans and continents. *Earth and Planetary Science Letters* **234**, 317–333.

Lomolino MV (2000) Ecology's most general, yet protean pattern: the species-area relationship. *Journal of Biogeography* **27**, 17–26.

López-Villalta JS (2016) Testing the predation-diversification hypothesis for the Cambrian–Ordovician radiation. *Paleontological Research* **20**, 312–321.

Lyle M (2015) Deep-sea sediments. Encyclopaedia of marine geosciences, 20pp, DOI 10.1007/978-94-007-6644-0_53-2. Available at https://link.springer.com/content/pdf/10.1007%2F978-94-007-6644-0_53-2.pdf.

Monnereau M and Cazenave A (1990) Depth and geoid anomalies over oceanic hotspot swells: a global survey. *Journal of Geophysical Research* **95**, 15429–15438.

Müller RD, Sdrolias M, Gaina C, Steinberger B and Heine C (2008) Basin dynamics long-term sea-level fluctuations driven by ocean. *Science (New York, N.Y.)* **319**, 1357–1362.

Munnecke A, Calner M, Harper DAT and Servais T (2010) Ordovician and Silurian sea–water chemistry, sea level, and climate: a synopsis. *Palaeogeography, Palaeoclimatology, Palaeoecology* **296**, 389–413.

Musiol S, Holohan EP, Cailleau B, Platz T, Dumke A, Walter TR, Williams DA and van Gasselt S (2016) Lithospheric flexure and gravity spreading of Olympus Mons volcano, Mars. *Journal of Geophysical Research: Planets* **121**, 255–272.

Neigel JE (2003) Species-area relationship and marine conservation. *Ecological Applications* **13**, 138–145.

Niu Y (1997) Mantle melting and melt extraction processes beneath ocean ridges: evidence from abyssal peridotites. *Journal of Petrology* **38**, 1047–1074.

Niu Y, Shi X, Li T, Wu S, Sun W and Zhu R (2017) Testing the mantle plume hypothesis: an IODP effort to drill into the Kamchatka-Okhotsk Sea basement. *Science Bulletin* **62**, 1464–1472.

Olson P, Reynolds E, Hinnov L and Goswami A (2016) Variation of ocean sediment thickness with crustal age. *Geochemistry, Geophysics, Geosystems* **17**, 1349–1369.

Paterson JR, Edgecombe GD and Lee MSY (2019) Trilobite evolutionary rates constrain the duration of the Cambrian explosion. *Proceedings of the National Academy of Sciences of the USA* **116**, 4394–4399.

Percival LME, Davies JHFL, Schaltegger U, De Vleeschouwer D, Da Silva A-C and Föllmi KB (2018) Precisely dating the Frasnian–Famennian boundary: implications for the cause of the Late Devonian mass extinction. *Nature Scientific Reports* **8**, 9578.

Peters SE and Gaines RR (2012) Formation of the 'great unconformity' as a trigger for the Cambrian explosion. *Nature* **484**, 363–366.

Philippot P, Ávila J, Killingsworth B, Killingsworth BA, Tessalina S, Baton F, Caquineau T, Muller E, Pecoits E, Cartigny P, Lalonde SV, Ireland TR, Thomazo C, van Kranendonk MJ and Busigny V (2018) Globally asynchronous sulphur isotope signals require re-definition of the great oxidation event. *Nature Communications* **9**, 2245.

Pistone K, Eisenman I and Ramanathan V (2019) Radiative heating of an ice-free Arctic ocean. *Geophysical Research Letters* **46**, 7474–7480.

Pitman WC (1978) Relationship between eustasy and stratigraphic sequences of passive margins. *Geological Society of America Bulletin* **89**, 1389–1403.

Portenga EW and Bierman PR (2011) Understanding Earth's eroding surface with ^{10}Be. *GSA Today* **21**, 4–10.

Rahbek C, Borregaard MK, Colwell RK, Dalsgaard B, Holt BG, Morueta-Holme N, Nogues-Bravo D, Whittaker RJ and Fjeldså J (2019) Humboldt's enigma: what causes global patterns of mountain biodiversity? *Science (New York, N.Y.)* **365**, 1108–1113.

Ramalho R, Helffrich G, Cosca M, Vance D, Hoffmann D and Schmidt DN (2010) Episodic swell growth inferred from variable uplift of the Cape Verde hotspot islands. *Nature Geoscience* **3**, 774–777.

Rosenblatt P, Pinet P and Thouvenot E (1994) Comparative hypsometric analysis of Earth and Venus. *Geophysical Research Letters* **21**, 465–468.

Rosing MT, Bird DK, Sleep NH and Bjerrum CJ (2010) No climate paradox under the faint early Sun. *Nature* **464**, 744–747.

Rozel AB, Golabek GJ, Jain C, Tackley PJ and Gerya T (2017) Continental crust formation on early Earth controlled by intrusive magmatism. *Nature* **545**, 332–335.

Sames B, Wagreich M, Conrad CP and Iqbal S (2020) Aquifer-eustasy as the main driver of short-term sea-level fluctuations during Cretaceous hothouse climate phases. *Geological Society, London, Special Publications* **498**, 9–38.

Saunders RS, Spear AJ, Allin PC, Austin RS, Berman AL, Chandlee RC, Clark J, Decharon AV, De Jong EM, Griffith DG, Gunn JM, Hensley S, Johnson WTK, Kirby CE, Leung KS, Lyons DT, Michaels GA, Miller J, Morris RB, Morrison AD, Piereson RG, Scott JF, Shaffer SJ, Slonski JP, Stofan ER, Thompson TW and Wall SD (1992) Magellan mission summary. *Journal of Geophysical Research: Planets* **97**, 13067–13090.

Schaefer L and Sasselov D (2015) The persistence of oceans on earth-like planets: insights from the deep-water cycle. *The Astrophysical Journal* **801**, 40 (13pp).

Scheffer M, Brovkin V and Cox P (2006) Positive feedback between global warming and atmospheric CO2 concentration inferred from past climate change. *Geophysical Research Letters* **33**, L10702.

Sim SJ, Stegman DR and Coltice N (2016) Influence of continental growth on mid-ocean ridge depth. *Geochemistry, Geophysics, Geosystems* **17**, 4425–4437.

Sleep NH (2007) Origins of the plume hypothesis and some of its implications. Book chapter, in *The Geological Survey of America*, 430, ISBN print: 9780813724300.

Smrekar SE and Stofan ER (1997) Corona formation and heat loss on Venus by coupled upwelling and delamination. *Science* **277**, 1289–1294.

Solé RV, Fernández P and Kauffman SA (2003) Adaptive walks in a gene network model of morphogenesis: insights into the Cambrian explosion. *The International Journal of Developmental Biology* **47**, 685–693.

Squire RJ, Campbell IH, Allen CM and Wilson CJL (2006) Did the Transgondwanan Supermountain trigger the explosive radiation of animals on Earth? *Earth and Planetary Science Letters* **250**, 116–133.

Squyres SW, Janes DW, Baer G, Bindschadler DL, Schubert G, Sharpton VL and Stofan ER (1992) The morphology and evolution of coronae on Venus. *JGR Planets* **97**, 13611–13634.

Stevenson DS and Wallace R (2021) Biogeographical modelling of exoplanets. *Astrobiology*, in press.

Stofan ER, Sharpton VL, Schubert G, Baer G, Bindschadler DL, Janes DL and Squyres SW (1992) Global distribution and characteristics of coronae and related features on Venus: implications for origin and relation to mantle processes. *Journal of Geophysical Research* **97**, 13347–13378.

Vodráqková S, Frýda J, Suttner TJ, Koptíková L and Tonarová P (2013) Environmental changes close to the Lower–Middle Devonian boundary; the Basal Choteč Event in the Prague Basin (Czech Republic). *Facies* **59**, 425–449.

Walker JCG, Hays PB and Kasting JF (1981) A negative feedback mechanism for the long-term stabilization of Earth's surface temperature. *Journal of Geophysical Research Atmospheres* **86**, 9776–9782.

Wei GY, Planavsky NJ, Tarhan LG, Chen X, Wei W, Li D and Ling H-F (2018) Marine redox fluctuation as a potential trigger for the Cambrian explosion. *Geology* **46**, 587–590.

Wheatley PJ, Louden T, Bourrier V, Ehrenreich D and Gillon M (2017) Strong XUV irradiation of the Earth-sized exoplanets orbiting the ultracool dwarf TRAPPIST-1. *Monthly Notices of the Royal Astronomical Society* **465**, L74–L78.

Williams JJ, Mills BJW and Lenton TM (2019) A tectonically driven Ediacaran oxygenation event. *Nature Communications* **10**, 2690.

Wilson DJ, Peirce C, Watts AB, Grevemeyer I and Krabbenhoeft A (2010) Uplift at lithospheric swells – I: seismic and gravity constraints on the crust and uppermost mantle structure of the Cape Verde mid-plate swell. *Geophysical Journal International* **182**, 531–550.

Wilson DJ, Peirce C, Watts AB and Grevemeyer I (2013) Uplift at lithospheric swells – II: is the Cape Verde mid-plate swell supported by a lithosphere of varying mechanical strength? *Geophysical Journal International* **193**, 798–819.

Wood R, Liu AG, Bowyer F, Wilby PR, Dunn FS, Kenchington CG, Cuthill JFY, Mitchell EG and Penny A (2019) Integrated records of environmental change and evolution challenge the Cambrian Explosion. *Nature Ecology & Evolution* **3**, 528–538.

Yakubchuk AS (2019) From Kenorland to modern continents: tectonics and metallogeny. *Geotecton* **53**, 169–192.

Zahnle K, Arndt N, Cockell C, Halliday A, Nisbet E, Selsis F and Sleep NH (2007) The emergence of a habitable planet. *Space Science Reviews* **129**, 35–78.

Zhang K (1998) *Twentieth Century Storm Activity and Sea Level Rise Along the U.S. East Coast and their Impact on Shoreline Position* (Ph.D. Thesis). University of Maryland, College Park, MD, 266.

Zhang K, Douglas BC and Leatherman SP (2004) Global warming and coastal erosion. *Climatic Change* **64**, 41–58.

Zhong S, Ritzwoller M, Shapiro N, Landuyt W, Huang J and Wessel P (2007) Bathymetry of the Pacific plate and its implications for thermal evolution of lithosphere and mantle dynamics. *Journal of Geophysical Research* **112**, 0148–0227.